Desalination and Water Treatment
www.deswater.com

doi: 10.5004/dwt.2020.24867

174 (2020) 389–399
January

Removal of TURQUOISE GN from aqueous solution using graphene oxide

Dewan Md. Mahmudunnabi, Md. Zahangir Alam, Md. Nurnabi*

Department of Applied Chemistry and Chemical Engineering, University of Dhaka, Dhaka 1000, Bangladesh, emails: nnabi@du.ac.bd (Md. Nurnabi), dmmnabidu@gmail.com (D. Md. Mahmudunnabi), zahangir@du.ac.bd (Md. Zahangir Alam)

Received 21 April 2019; Accepted 8 September 2019

ABSTRACT

In this study, graphene oxide (GO) was prepared from graphite powder by modified Hummers' method. Characterization of prepared GO was carried out by FTIR, Raman spectroscopy, SEM, AFM, XRD and elemental analysis. To observe its adsorption capacity, it was applied for adsorption of a synthetic anionic dye, TURQUOISE GN (TGN) used in textile industries. The influence of pH, dosage of adsorbent, time, concentration of the dye on adsorption capacity of GO were studied. The experimental results showed that GO can be used as a promising adsorbent for dye removal from textile effluents. The distribution of TGN on GO was determined by applying Langmuir as well as Freundlich isotherm models and the results match preferably with Langmuir model. The theoretical maximum sorption capacities were determined from Langmuir isotherm which were 565.61 and 294.12 mg/g at pH of 2 and 7, respectively. To find out the mechanism of TGN adsorption on GO, pseudo-first-order as well as pseudo-second order models were applied and the results matched well with second-order model. From thermodynamic effect, it was found that the adsorption process is more spontaneous at lower temperature and it is a physisorption process. The regeneration of the used GO was studied and found that regenerated GO showed about 40% adsorption efficiency with respect to fresh GO up to 4th recycle for the removal of TGN from aqueous solution.

Keywords: Graphite; Graphene oxide; Hummers' method; Zeta potential; Adsorption capacity

1. Introduction

For the last few decades, textile industries have been playing a vital role in the development of Bangladesh's economy. According to Bangladesh Textile Mills Association at present, there are about 1,461 textile related industries in Bangladesh that provide more than 5 million of skilled and unskilled people employment of which about 80% are women. These employment accounts 45% of all industrial employment and contributes more than 12% of total GDP of Bangladesh. So, this sector is extremely important for the national economy as well as for socioeconomic development of Bangladesh. In spite of these importance, textile sector creates a huge problem to our environment by directly discharging effluents containing dyes. More than 100,000 commercially dyes are available and 7×10^5 ton of dye-stuffs are produced annually in the world. About 10% of the used dyes are subsequently lost during the textile coloration process and more or less 2% of used dye are discharged directly into the effluent [1,2]. Dyes are highly colored, stable to light, non-degradable, toxic and cause harm to human and other living beings by entering into food chain. Dyes affect human immune system and cause skin irritation, respiratory sensitization, watery eyes, sneezing and symptoms of asthma [3,4]. For the treatment of textile effluents some physical as well chemical or biological methods are generally used [5]. Among these methods adsorption gives the best result to remove coloring materials from effluents. Activated carbon shows very high adsorption capacity and is generally used as adsorbent, but owing to high cost it is not well accepted by the industrialists [6,7]. Moreover, regeneration of saturated activated carbon is very difficult and also non-selective, non-effective to vat or disperse dyes [8]. For dye adsorption,

---

* Corresponding author.

1944-3994/1944-3986

some less expensive, non-conventional abundant adsorbents such as peat [9,10], bagasse [11,12], rice straw [13], rice husk [14,15], sawdust [16,17], fly ash [18,19], clay materials [20,21] were also used. The adsorbents are very cheap and abundant but demonstrated comparatively low adsorption capacity, required high retention time and their regeneration is difficult.

Different biological treatment processes are claimed to be more economical compared with other physical and chemical methods in this purpose [22,23]. But drawbacks of these methods are enormous, such as requirement of large land area, high retention time, low adsorption capacity, pH and temperature dependency. Some chemicals used in this process are toxic, complex in structure and obtained from synthetic organic origin [24]. Some dyes are recalcitrant to this treatment and due to xenobiotic nature total degradation of azo dyes are not possible. Another traditional method used for dye removal from effluent is coagulation–flocculation method [25]. But there are also some drawbacks of this process such as lack of versatility, requiring varying coagulant dose, low dye removal capacity, etc. It also needs large land area, forms too much sludge and very much pH dependent [26].

Recently, some research groups reported that graphene and its derivatives showed excellent results in removing dyes [27–31] or both dyes and heavy metals [32,33] from their aqueous solutions because of its high surface area. But the preparation of GO is very costly and they are applied for the removal of model dyes, mainly for cationic dyes [27,28,31,32]. So, still there are some scope to develop technique for the synthesis of GO and its derivatives which will be attractive as well as economically viable adsorbents for the removal of variety of dyes. In our research, very cheap graphite powder was used for the synthesis of GO and applied for the removal of TURQUOISE GN (Copper,[29H,31H-phthalocyaninato(2)-N29,N30,N31,N32]-,sulfo[[4-[[(sulfooxyl)ethyl]sulfonyl] phenyl]amino]sulfonyl) from aqueous solution. TURQUOISE GN is an anionic reactive dye and also known as reactive blue 21 (M.F-$C_{40}H_{25}CuN_9O_{14}S_5$ and M.W-1,079.535 g/mol) [34]. It is commercially available and widely used in textile dyeing processes.

2. Experimental

2.1. Materials

TGN dye (CAS-No: 73049-92-0) was collected from Interstoff Apparels Ltd, Gazipur, Bangladesh, and the chemical structure of it is shown in Fig. 1. Graphite powder (≤50 μm 99.5%) was used for the synthesis of GO. The chemicals used were H_2O_2 (30%), H_2SO_4 (98%), HNO_3 (65%), $KMnO_4$, $NaNO_3$ and HCl (37%). Graphite powder and H_2O_2 were bought from Merck (India), H_2SO_4 and HNO_3 from Active Fine Chemicals (Bangladesh), $KMnO_4$ from Merck (Germany), $NaNO_3$ from Uni-chem (China) and HCl from RCI Labscan (Thailand). All these chemicals were of analytical grade and used as received.

2.2. Synthesis of graphene oxide

Modified Hummers' method was used for the synthesis of GO [35]. Briefly, 3.0 g of graphite powder was dispersed in a mixture of 75 mL concentrated H_2SO_4 and HNO_3 in the ratio of 3:1 with vigorous stirring. After 2 h of stirring, 9.0 g of $KMnO_4$ and 1.5 g of $NaNO_3$ were added to the mixture and the mixture was stirred overnight. Then 90 mL of deionized (DI) water was added to the thick paste with continuous stirring. When the color of the mixture changed to deep brown, 300 mL of DI water, 20 mL of 30% H_2O_2 and 200 mL of 5% HCl were added with continuous stirring. After addition of H_2O_2, the color of the mixture changed to bright yellow. Finally, the GO mixture was washed several times with distilled water until its pH reached to 7.0.

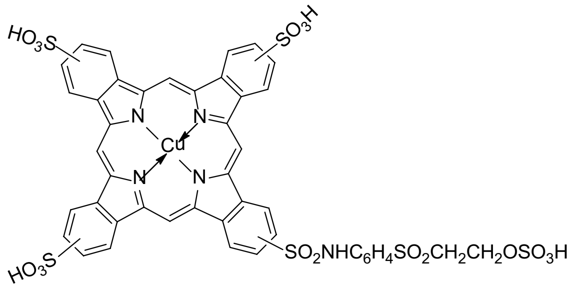

Fig. 1. Structure of dye Turquoise GN.

2.3. Characterization methods

Composition of GO was determined by elemental analysis with Vario Micro CHNS. The chemical structures of graphite and GO were studied with Fourier transformed infrared (FTIR) spectrophotometer (IR Prestige-21, SHIMADZU, Japan). The morphology and microstructure of GO were studied with SEM (JSM-6010 PLUS/LA). The height of the prepared GO layer was measured by atomic forced microscopy, AFM (Nanosurf Acoustic Enclosure 100, Department of Physics, University of Dhaka). X-ray diffraction of graphite and GO was performed on Multipurpose X-ray diffraction system (Ultima IV) with Cu Kα radiation ($\lambda = 0.154$ nm, 40 kV, 1.64 mA) in the range 5°–100°. The presence of D-band and G-band in GO was determined by the Raman spectroscopy (MonoVista CRS+). The zeta potential value at different pH was measured using Malvern Zetasizer Nano-ZS analyser (Materials Science Division, Atomic Energy Centre, Dhaka).

2.4. Adsorption study

In the adsorption of TGN on GO, the effects of various parameters such as pH, dosage of adsorbent, initial concentration of dye, contact time were investigated to explore the optimum conditions. The pH effects were carried out at a range of 2–10 and dosage effects were carried out at 5–20 mg GO per 10 mL dye solution. The duration of the experiments varied from 2 to 60 min with various concentration and the mixtures were stirred at 200 rotations per minute. The change of dye concentration after adsorption was determined by spectrophotometric method (UV-1700 Pharma Spec UV-VIS Spectrophotometer, SHIMADZU, Japan). The absorbance was determined at 660 nm with respect to a standard curve (5–200 ppm). The following equation was used to calculate adsorption capacity q (mg/g):

$$q = \frac{(C_0 - C_t) \times V}{W} \tag{1}$$

where C_0 = initial concentration of dye (ppm), V = volume of the dye solution (L), C_t = concentration of dye (ppm) at time t, W = mass of the adsorbent (g).

The equilibrium adsorption capacity q_e (mg/g) was calculated by equation as follows:

$$q_e = \frac{(C_0 - C_e) \times V}{W} \tag{2}$$

where C_e = concentration of dye (ppm) at equilibrium condition.

The % of dye removal was calculated by the formula as follows:

$$\% \text{ removal} = \frac{(C_0 - C_t) \times 100}{C_0} \tag{3}$$

The Langmuir and Freundlich isotherm models were applied to study the distribution of dye on GO surface. For monolayer distribution, Langmuir isotherm Eq. (4) was employed.

$$\frac{C_e}{q_e} = \frac{1}{q_m b} + \frac{1}{q_m} C_e \tag{4}$$

where C_e = equilibrium concentration, q_e = equilibrium adsorption capacity, q_m = theoretical maximum adsorption capacity, b = Langmuir constant.

The separation factor R_L is related to Langmuir constant b through the equation

$$R_L = \frac{1}{1 + C_m b} \tag{5}$$

where C_m = dye concentration (maximum).

The following Freundlich isotherm Eq. (6) was used for the present study:

$$\ln q_e = \ln k_F + \frac{1}{n} \ln C_e \tag{6}$$

Adsorption kinetics was tested by the following pseudo-first order Eq. (7) and pseudo-second order Eq. (8) kinetics.

$$\log(q_e - q_t) = \log q_e - \frac{k_1}{2.303} t \tag{7}$$

where q_e and q_t are adsorption capacity at time t and at equilibrium.

$$\frac{t}{q_t} = \frac{1}{k_2 q_{e^2}} + \frac{1}{q_e} t \tag{8}$$

where k_1 and k_2 are rate constants of pseudo-first order and pseudo-second order adsorption.

The changes in Gibb's free energy for dye adsorption on graphene oxide at different temperature were calculated by Eq. (9) as follows:

$$\Delta G^\circ = -RT \ln k_d \tag{9}$$

where k_d = distribution constant, R = universal gas constant (8.314 J mol^{-1} K^{-1}) and T = absolute temperature (K). K_d was calculated by using Eq. (10) as follows:

$$k_d = \frac{q_e}{C_e} \tag{10}$$

The average standard enthalpy change ΔH^o and entropy change ΔS^o for the adsorption was calculated by Van't Hoff equation as follows:

$$\ln k_d = \frac{-\Delta H^o}{RT} + \frac{\Delta S^o}{R} \tag{11}$$

3. Results and discussion

3.1. Characterization of prepared GO

Composition of GO was determined by elemental analysis and found to contain 40.99% C, 3.09% H, 4.08% N and 0.40% S. It was also found to contain a considerable amount of oxygen (51.44%) that was determined indirectly. The elemental analysis data were in good agreement with the literature [36].

The functional groups present in graphite and GO were studied with FTIR spectroscopic analysis. From Fig. 2a, it was evident that for GO vibrational peaks were observed at 1,080; 1,412; 1,620; 1,708; 2,919 and 3,408 cm^{-1} attributable to C–O, carboxy C–O, aromatic C=C, carbonyl C=O, C–H stretching and –OH stretching groups, respectively [37,38]. These data indicate the presence of –COOH group in GO while the peaks were absent in case of graphite powder. Thus it was evident that graphite powder was oxidized to graphene oxide under the reaction protocol.

Raman spectrum of GO is shown in Fig. 2b that confirmed the existence of both the D-band and G-band where G-band is located at 1,569 cm^{-1} and the D-band is located at 1,340 cm^{-1}. Similar locations of these bands are observed in the literature published elsewhere [37]. The existence of D-band revealed the presence of defect sites in the GO sheets and the size of the in-plane sp^2 domain [39].

The morphology and microstructure of GO were studied with SEM and image in Fig. 3 shows a fluffy structure with many wrinkles. It is assumed that the fluffiness and wrinkles in the GO are due to oxidation and layer separation.

To determine the thickness of the prepared GO layer, the sample was prepared by drop-casting onto a glass substrate. From the AFM image of GO (Fig. 4a) and the section line analysis (Fig. 4b), the thickness was found to be 7.37 nm. From the results, it can be assumed that the prepared film is formed by multilayer GO deposition [40].

The XRD patterns of graphite and GO are represented in Fig. 5. A sharp and strong peak was observed at 2θ = 26.73° for graphite powder corresponding to an interlayer spacing of

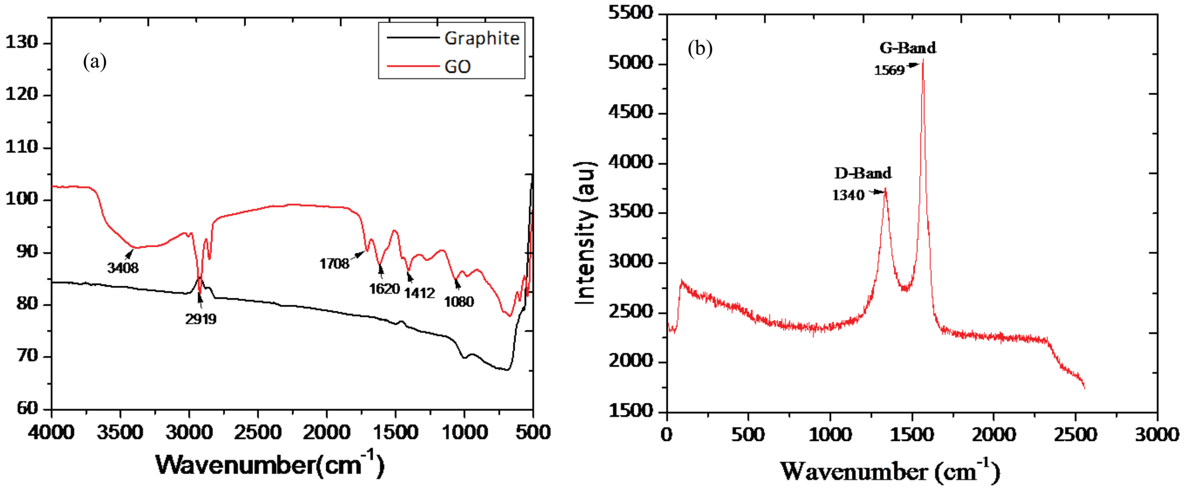

Fig. 2. FTIR spectra of graphene oxide and graphite powder (a) and Raman spectrum of GO (b).

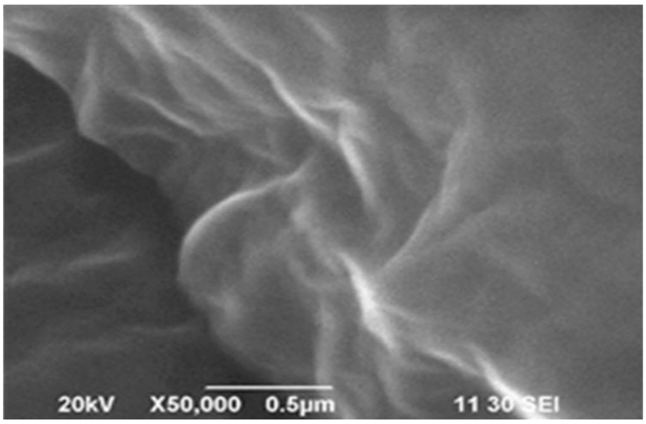

Fig. 3. SEM image of GO.

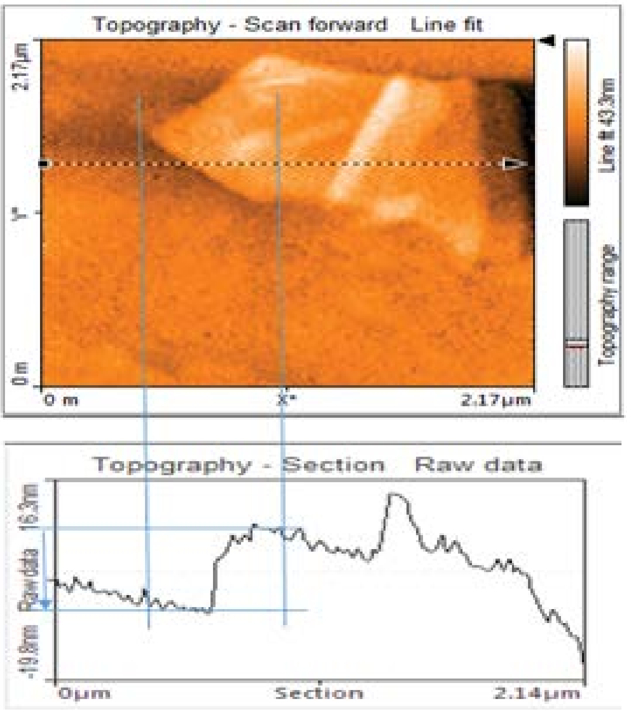

Fig. 4. AFM height image (a) and the section line analysis (b) of GO.

3.33 Å, while for GO a broad peak was observed at 2θ = 9.97° and interlayer spacing was 8.87 Å. The shift of the peak of GO compared with graphite powder is assumed due to the damage of the crystalline structure of graphite resulting in the formation of amorphous structure and introduction of oxygen [41,42].

Zeta potential of GO at different pH (Fig. 6) was also studied. For this study, GO sample was prepared by dispersing GO in DI water. The analysis was carried out in the pH range of 2–10 and the values were negative over the whole pH range. The negative values increase from –18.1 to –36 mV when pH increases from 2 to 10. This type of charge was also found in some documented literature [43].

3.2. Effect of different operational parameters on adsorption capacity of GO

3.2.1. Effect of pH on adsorption capacity of GO

pH has great influence on the surface charge of GO and dye molecule. So, it is a very important parameter to determine the adsorption capacity of prepared GO. The effects of pH on adsorption of GO were studied at the range of 2–10. In these studies, 10 mg of disperse GO were added in each solution and the mixtures were shaken for 60 min at 200 rpm. Then the mixtures were filtered and changes in concentrations were determined by UV-Vis spectroscopy. Maximum adsorption capacity of GO was 161.98 mg/g (Fig. 7) at pH of 2 and it decreased with an increase in pH.

It is assumed that at higher pH, carboxylic groups of GO dissociated extensively and surface of GO became highly negatively charged [44], while at higher pH the dye molecule existed as anion (dye$^-$) which is more water soluble and underwent electrostatic repulsion with the negatively charged surface of GO and thus resulted lower adsorption. On the other hand, at low pH some of the carboxyl groups

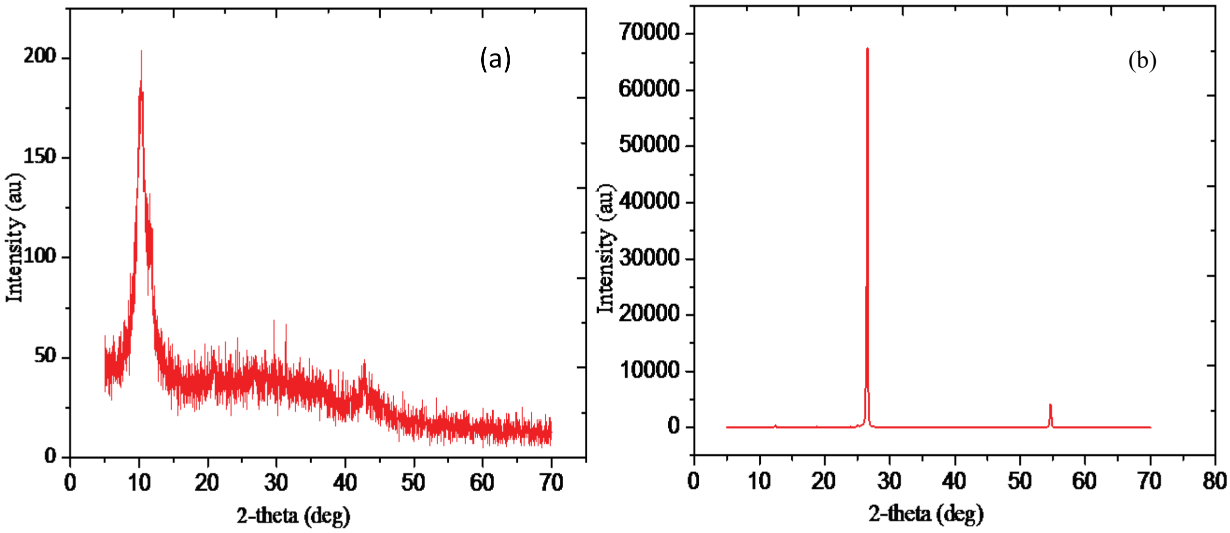

Fig. 5. XRD patterns of GO (a) and graphite (b).

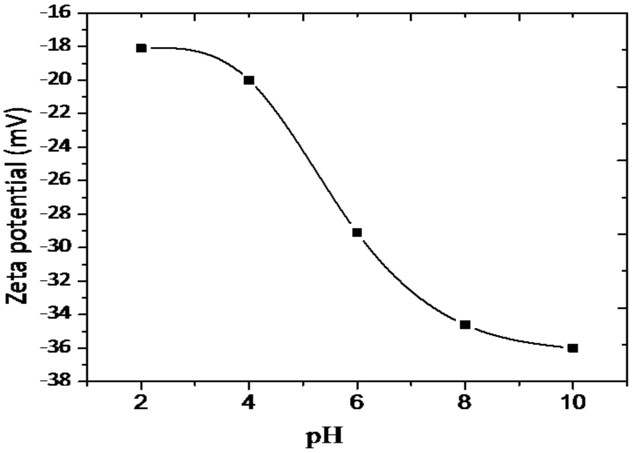

Fig. 6. Zeta potential of GO vs. pH.

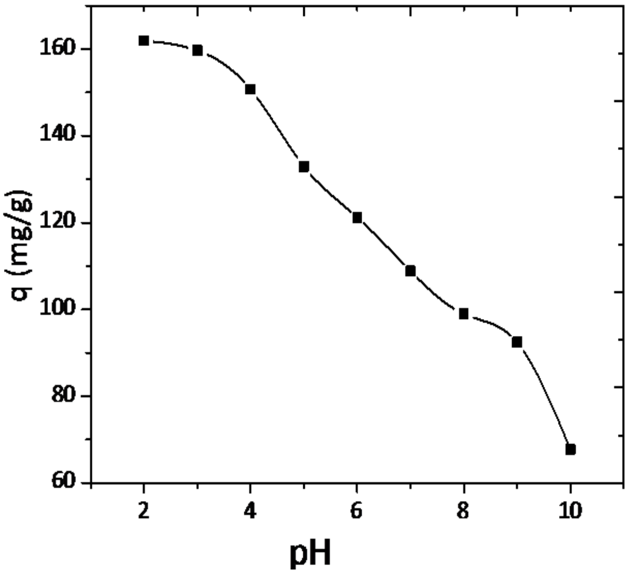

Fig. 7. Effects of solution pH on adsorption capacity of GO (200 ppm dye solution, temperature: 303 K; dosage: 10 mg/10 mL solution).

of GO was protonated and formed positive ions [45] and demonstrated electrostatic attraction between anionic dye and adsorbent, which led to the higher adsorption.

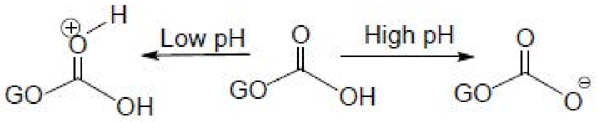

$$\text{Dye-SO}_3\text{H} \underset{\text{Lower pH}}{\overset{\text{Higher pH}}{\rightleftharpoons}} \text{Dye-SO}_3^-$$

3.2.2. Effect of dosage of GO on adsorption capacity

The effects of dosage on adsorption of dye were also studied. Optimization of the dose of adsorbent was carried out using 300 ppm solution at pH of 2. The process was carried out for 10 min with the adsorbents with a dosage of 5–20 mg. It is apparent that (Fig. 8) with the increase of adsorbent dosage adsorption capacity decreased but percentage removal of dye increased. It is readily understood that with the increase of adsorbent dose, the amount of adsorbate per unit mass of adsorbent decreased [46]. It was observed that a dosage of 9 mg/10 mL solution demonstrates the best percentage removal as well as the best adsorption capacity. However for simplicity 10 mg/10 mL solution dosage was maintained throughout the study.

3.2.3. Effect of dye concentration and contact time on adsorption capacity

The effect of dye concentration and contact time on adsorption capacity of GO was also studied. For this 10 mL solutions of different concentrations were taken in a conical flask and 10 mg of disperse GO were added to each solution. This study revealed that maximum adsorption capacity of GO was achieved at pH of 2. In addition, pH of effluents generally ranges from 7 to 8. Therefore, the adsorption experiments were carried out at a pH of 2 and pH of 7 in the time range 2–60 min. The results showed that (Fig. 9) adsorption capacity increased with an increase of time until it reached at equilibrium and became constant. The reason is, at the beginning more active sites were available and with the increase of time these sites became saturated. As a result, the adsorption capacity became constant. If initial dye concentration increases equilibrium adsorption capacity also increases because of increase in concentration gradient between the dye molecules in the bulk solution [47]. This results in mass transfer between the dye solution and adsorbent.

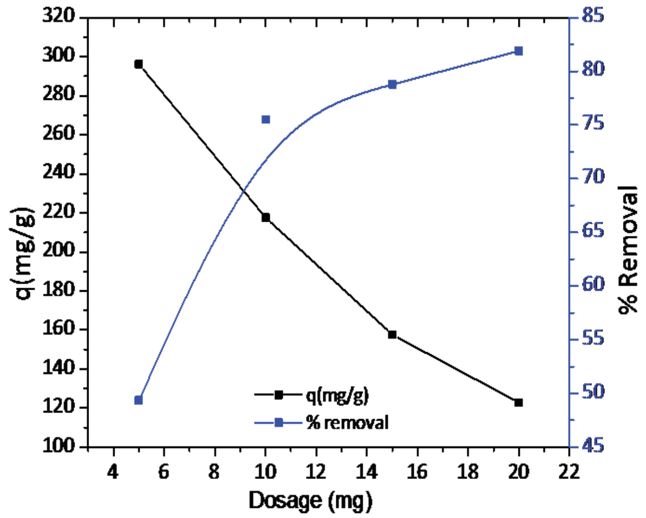

Fig. 8. Effects of dosage of GO (mg/10 mL solution) on 300 ppm dye solution at pH of 2 and 303 K temperature.

3.3. Adsorption isotherms

Distribution of dye molecules on GO surface can be investigated using Langmuir and Freundlich isotherms. Langmuir isotherm gives assumption about monolayer adsorption with no interaction between the adsorbate molecules [48], whereas, Freundlich isotherm gives assumption about multilayer non-uniform adsorption [49].

Langmuir model was tested by plotting C_e/q_e vs. C_e (Fig. 10). A linear relation between C_e/q_e and C_e was observed for both adsorptions at pH of 2 and pH of 7 with acceptable regression factor. Theoretical maximum sorption capacities, q_m calculated from the slope were found to be 565.61 mg/g and 294.12 mg/g at pH of 2 and pH of 7, respectively. The separation factor, R_L between 0 and 1 indicates the suitability of monolayer adsorption [31]. In this study, R_L values of 0.67 and 0.236 at pH of 2 and pH of 7, respectively, indicates a very favorable monolayer adsorption.

The experimental data were also tested by Freundlich isotherm; plotting $\ln C_e$ vs. $\ln q_e$ (Fig. 11) and linear relationship was observed. The value of n was calculated using Eq. (6) and found to be 1.81 and 2.05 at pH of 2 and pH of 7, respectively, which showed that the adsorption was moderate to good. The value of n between 2 and 10 indicates good adsorption and 1–2 indicates difficult adsorption [31].

The values of different parameters of Langmuir and Freundlich models are provided in Table 1 and the values indicate that the adsorption of TGN on GO matches well with Langmuir model.

The adsorption capacity of the prepared GO is quite significant. To evaluate the adsorption ability of the prepared adsorbent, the result is compared with previous works on graphene-based adsorbents for the removal of dyes (Table 2).

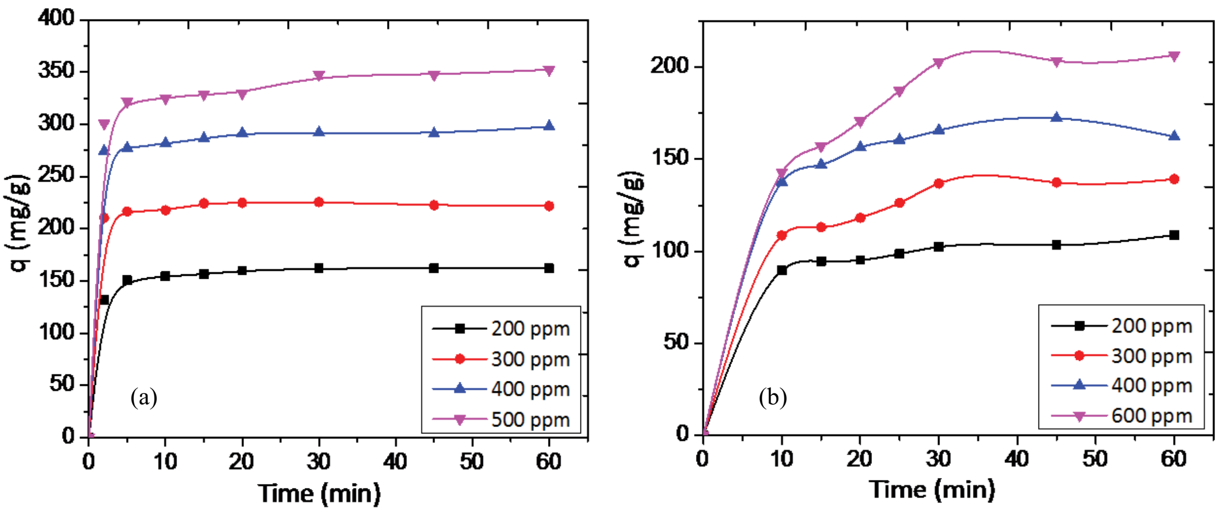

Fig. 9. Effect of concentration and time on adsorption capacity of GO at the dosage of 10 mg /10 mL dye solution at pH of 2 (a) and pH of 7 (b), respectively at 303 K.

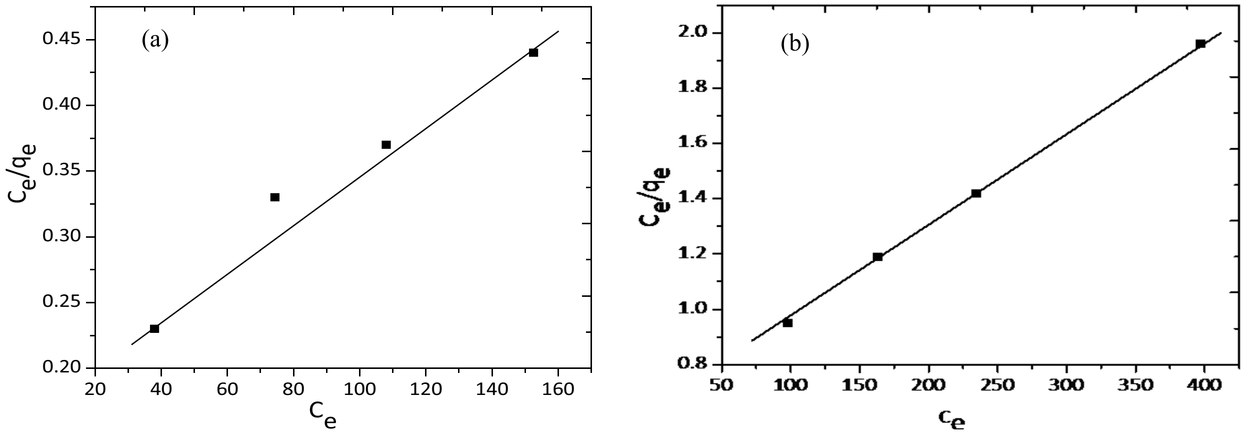

Fig. 10. Langmuir adsorption isotherm at 303 K temperature at pH of 2 (a) and pH of 7 (b), respectively.

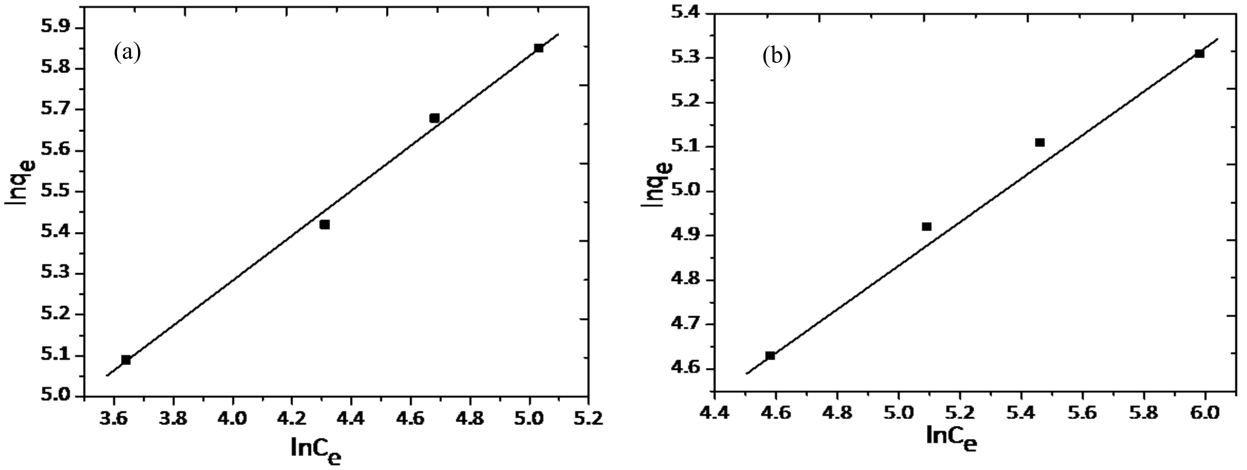

Fig. 11. Freundlich adsorption isotherm at 303 K temperature at pH of 2 (a) and pH of 7 (b), respectively.

Table 1
Theoretical values of q_m, b, R_L, n, K_F and R^2

Name of isotherm	Langmuir isotherm				Freundlich isotherm		
	q_m (mg/g)	R^2	b, L mg^{-1}	R_L	R^2	n	K_F
At pH of 2	565.61	0.969	0.0010	0.670	0.996	1.81	21.43
At pH of 7	294.12	0.999	0.0054	0.236	0.993	2.05	11.25

3.4. Adsorption kinetics

To evaluate the underlying mechanisms of adsorption, the pseudo-first-order and pseudo-second-order kinetics were also studied. In 1998, Lagergren presented first-order model which is obtained by plotting $\log(q_e–q_t)$ vs. t (Fig. 12) and there is a linear relationship between $\log(q_e–q_t)$ and t.

Ho and Mckay [50] presented a pseudo-second order model which is obtained by plotting t/q_t vs. t (Fig. 13).

From Table 3 it is observed that the calculated adsorption capacities of second-order kinetics matched well with the experimental values and the values of correlation coefficient are also better for second-order kinetics. So, the adsorption of TGN onto GO follows the pseudo-second-order model.

3.5. Thermodynamic analysis

The changes in Gibb's free energy for dye adsorption on graphene oxide at different temperatures were also studied. In this case, 10 mg GO was added to 10 mL 200 ppm dye solution at a pH of 2 for each experiment. The mixtures were shaken at 303, 313 and 323 K for different time periods ranging from 5 to 60 min. The effects of contact time and

Table 2
Some of graphene-based adsorbents with their adsorption capacity

Name of the adsorbent	Adsorption capacity	References
Graphene	30.32 mg g^{-1} for Basic Red 46	[51]
Graphene oxide	55.57 mg g^{-1} for Basic Red 46	
Single-walled carbon nanotubes	38.35 mg g^{-1} for Basic Red 46	
Carboxylate group functionalized single-walled carbon nanotubes	49.45 mg g^{-1} for Basic Red 46	
Superparamagnetic graphene oxide-Fe$_3$O$_4$ hybrid composite	167.2 mg g^{-1} for methylene Blue and 171.3 mg g^{-1} for Neutral Red.	[28]
Thermally reduced graphene (TRG)	89.3 mg g^{-1} for Methyl Orange	[31]
Magnetic graphene oxide	64.23 mg g^{-1} for methylene blue and 20.85 mg g^{-1} for orange G	[32]

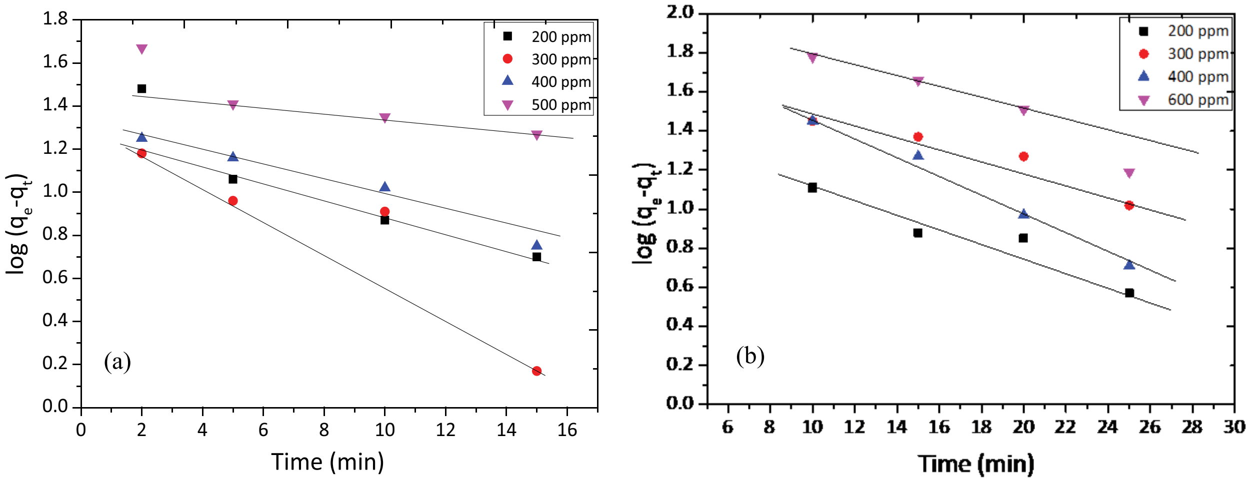

Fig. 12. Pseudo-first order adsorption kinetics at pH of 2 (a) and pH of 7 (b), respectively, at 303 K.

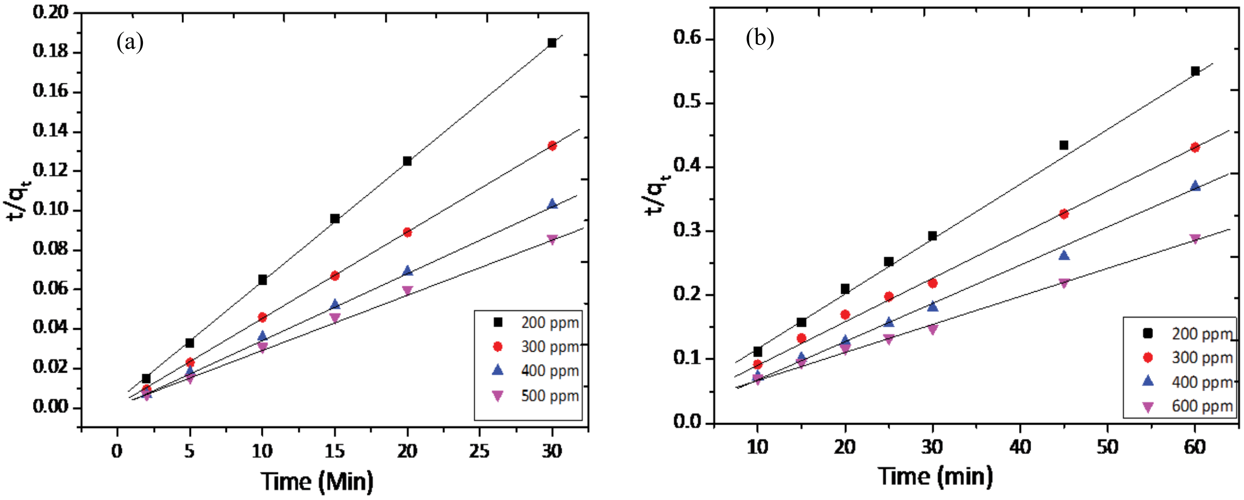

Fig. 13. Pseudo-second order adsorption kinetics at pH of 2 (a) and pH of 7 (b), respectively, at 303 K.

temperature on adsorption of TGN on GO were also studied and are plotted in Fig. 14a. The adsorption capacities of GO were decreased when the temperatures were increased. This is because the kinetic energy increases with temperature and which results in release of the adsorbate from GO. The equilibrium adsorption capacity was 162.03 mg/g at 303 K that

Table 3
Pseudo-first-order and pseudo-second-order kinetics parameters

Types of kinetics model	Parameters	Results at pH of 2				Results at pH of 7			
		200 ppm	300 ppm	400 ppm	500 ppm	200 ppm	300 ppm	400 ppm	600 ppm
Pseudo-first order	$q_{e,\exp}$, mg/g	162.00	225.61	291.96	347.39	102.39	136.84	165.66	202.86
	$q_{e,\mathrm{cal}}$, mg/g	30.27	23.55	22.18	40.18	26.92	58.08	95.94	161.06
	K_1, 1/min	0.13	0.16	0.085	0.046	0.076	0.064	0.116	0.088
	R^2	0.947	0.851	0.972	0.787	0.9268	0.9229	0.99	0.9438
Pseudo-second order	$q_{e,\mathrm{cal}}$, mg/g	163.67	227.27	293.17	350.88	113.64	151.52	172.41	232.56
	K_2, g/mg min	0.0122	0.0173	0.043	0.01	0.0027	0.0015	0.0030	0.0007
	R^2	1.0	0.999	0.999	0.999	0.9986	0.9976	0.9955	0.9967

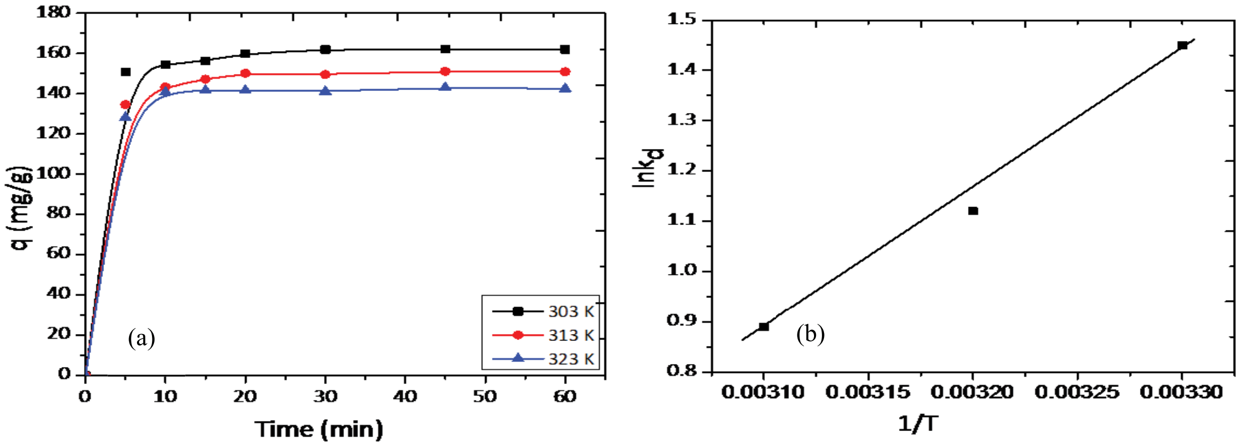

Fig. 14. Effects of temperature on adsorption capacity of GO (a) and 1/T vs. lnk_d plot (b). Dose: 10 mg/10 mL; concentration: 200 ppm, pH = 2.

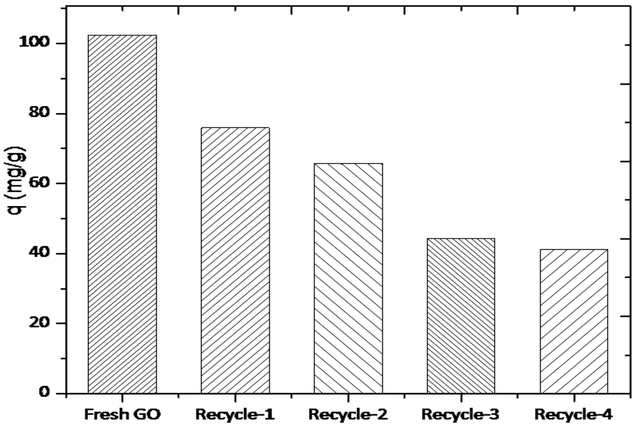

Fig. 15. Reusability of GO for the removal of TGN at the dosage of 10 mg/10 mL 200 ppm solution at pH of 7.

decreased to 150.80 and 141.65 mg/g at 313 and 323 K, respectively. The Gibb's free energies calculated with Eq. (10) were found to be –3.66, –2.92, –2.39 kJ mol^{-1} at 303, 313 and 323 K, respectively.

The average standard enthalpy change ΔH° and entropy change ΔS° for the adsorption was calculated from the Van't Hoff equation. A straight line was obtained by plotting ln k_d vs. 1/T (Fig. 14b). The standard enthalpy change ΔH° obtained from the slope, and the entropy change ΔS° obtained from the intercept were –23.28 kJ mol^{-1} and –0.065 kJ K^{-1} mol^{-1}, respectively. The value of ΔG° increased from –3.66 to –2.39 with increases of the temperature from 303 to 323 K. Thus the adsorption of TURQUOISE GN on GO was spontaneous at lower temperature. Moreover, Gibb's free energy also indicates the nature of adsorption, namely physical adsorption and chemisorptions. The ΔG° values in our experiments indicate that the adsorption of TGN on GO was a physical adsorption [31].

3.6. Plausible mechanism of adsorption

Generally hydrogen bonding, electrostatic or π–π interactions are main reasons of organic dye adsorption on graphene-based materials. Graphene oxide possesses negative surface charge and showed electrostatic as well as π–π interaction to cationic dye [52]. So, GO has more adsorption capacity to cationic dyes compared with anionic dyes. But in our study, the prepared GO also showed a significant adsorption of anionic dye. In this case, it is assumed that the adsorption of dye on GO may be due to its surface defects, hydrophobic GO–dye association, π–π interaction [52] as well as van der walls interactions [29].

3.7. Regeneration of used graphene oxide

Regeneration studies provide useful information for adsorption mechanism and commercial application of an adsorbent. In order to check the regeneration ability, the used GO was washed with 2% HCl solution. Then neutralized through washing with distilled water and used for further adsorption. In this study, 10 mg of dispersed regenerated GO was used for10 mL 200 ppm dye solution at pH of 7 with shaking for 30 min. Fresh GO showed the adsorption capacity of 102.39 mg/g for 200 ppm dye solution at pH of 7 while the regenerated GO of 1st, 2nd, 3rd and 4th recycle (Fig. 15) show the adsorption capacities of 75.91, 65.73, 44.32 and 41.25 mg/g, respectively.

4. Conclusions

From the above analyses, it can be concluded that the prepared graphene oxide is so effective for the removal of anionic dyes. The optimum conditions for the maximum adsorption were a pH of 2 and 9 mg dosage per 10 mL dye solution at a temperature of 303 K. Adsorption capacities of the prepared GO were 565.61 and 294.12 mg/g at pH of 2 and pH of 7, respectively. Adsorption of TGN on GO followed both the Langmuir isotherm and Freundlich isotherm but preferably Langmuir isotherm. The pseudo-second order kinetic model gives a better correlation for the adsorption of dye onto graphene oxide compared with the pseudo-first-order model. The observed value of Gibb's free energy (ΔG^o) is negative indicating a spontaneous physical adsorption of TGN on GO. Consequently, the used GO can be regenerated and showed about 40% adsorption efficiency with respect to fresh GO up to 4th recycle.

Acknowledgment

The authors acknowledge the financial support from the University Grants Commission of Bangladesh (Fellowship No.: BMK/Britti / 1.157/ MPhil and PhD/2016/5343).

References

[1] C.I. Pearce, J.R. Lioyd, J.T. Guthire, The removal of colour from textile wastewater using whole bacterial cells: a review, Dyes Pigm., 58 (2003) 179–196.

[2] T. Robinson, G. McMullan, R. Marchant, P. Nigam, Remediation of dyes in textile effluent : a critical review on current treatment technologies with a proposal alternative, Bioresour. Technol., 77 (2001) 247–255.

[3] C. O'Neill, F.R. Hawkes, D.L. Hawkes, N.D. Lourenco, H.M. Pinheiro, W. Delee, Colour in textile effluents–sources, measurement, discharge consents and simulation: a review, J. Chem. Technol. Biotechnol., 74 (1999) 1009–1018.

[4] M.A. Hassaan, A.E. Nemr, Health and environmental impacts of dyes: mini review, Am. J. Environ. Sci. Eng., 1 (2017) 64–67.

[5] S.M. Ghoreishi, R. Haghighi, Chemical catalytic reaction and biological oxidation for treatment of non-biodegradable textile effluent, Chem. Eng. J., 95 (2003) 163–169.

[6] A.K. Jain, V.K. Gupta, A. Bhatnagar, Suhas, Utilization of industrial waste products as adsorbents for the removal of dyes, J. Hazard. Mater., B101 (2003) 31–42.

[7] A. Dabrowski, Adsorption, from theory to practice, Adv. Colloid Interface Sci., 93 (2001) 135–224.

[8] G. Crini, Non-conventional low-cost adsorbents for dye removal: a review, Bioresour. Technol., 97 (2006) 1061–1085.

[9] R.M. Lattuada, M.C.R. Peralba, D. Santos, J.H.Z, A.G. Fisch, Peat, rice husk and rice husk carbon as low-cost adsorbents for metals from acidic aqueous solutions, Sep. Sci. Technol., 49 (2014) 101–111.

[10] Z.R. Liu, X. S. Chen, L.M. Zhou, P. Wei, Development of a first-order kinetics-based model for the adsorption of nickel onto peat, Min. Sci. Technol., 19 (2009) 230–234.

[11] M. Valix, W.H. Cheung, G. Mckay, Preparation of activated carbon using low temperature carbonisation and physical activation of high ash raw bagasse for acid dye adsorption, Chemosphere, 56 (2004) 493–501.

[12] J.C. Cueva-Orjuela, A.D. Hormaza-Anaguano, A. Merino-Restrepo, Sugarcane bagasse and its potential use for the textile effluent treatment, Dyna, 84 (2017) 291–297.

[13] N. Kannan, M.M. Sundaram, Kinetics and mechanism of removal of methylene blue by adsorption on various carbons-a comparative study, Dyes Pigm., 51 (2001) 25–40.

[14] M.M. Mohamed, Acid dye removal: comparison of surfactant-modified mesoporous FSM-16 with activated carbon derived from rice husk, J. Colloid Interface Sci., 272 (2004) 28–34.

[15] V.S. Mane, I.D. Mall, V.C. Srivastava, Kinetic and equilibrium isotherm studies for the adsorptive removal of Brilliant Green dye from aqueous solution by rice husk ash, J. Environ. Manage., 84 (2007) 390–400.

[16] M.W. Ashraf, N. Abulibdeh, A. Salam, Adsorption studies of textile Dye (Chrysoidine) from aqueous solutions using activated sawdust, Int. J. Chem. Eng., 2019 (2019) 1–9.

[17] S.R. Shukla, R.S. Pai, Adsorption of Cu(II), Ni(II) and Zn(II) on dye loaded groundnut shells and sawdust, Sep. Purif. Technol., 43 (2005) 1–8.

[18] M. Visa, C. Bogatu, A. Duta, Simultaneous adsorption of dyes and heavy metals from multicomponent solutions using fly ash, Appl. Surf. Sci., 256 (2010) 5486–5491.

[19] M. Visa, L. Andronic, D. Lucaci, A. Duta, Concurrent dyes adsorption and photo-degradation on fly ash based substrates, Adsorption, 17 (2011) 101–108.

[20] A. Gurses, S. Karaca, C. Dogar, R. Bayrak, M. Acikyildiz, M. Yalcin, Determination of adsorptive properties of clay/water system: methylene blue sorption, J. Colloid. Interface Sci., 269 (2004) 310–314.

[21] S. Wang, Y. Boyjoo, A. Choueib, Z.H. Zhu, Removal of dyes from aqueous solution using fly ash and red mud, Water Res., 39 (2005) 129–138.

[22] G. McMullan, C. Meehan, A. Conneely, N. Kirby, T. Robinson, P. Nigam, I.M. Banat, R. Marchant, W.F. Smyth, Microbial decolourisation and degradation of textile dyes, Appl. Microbiol. Biotechnol., 56 (2001) 81–87.

[23] I.M. Banat, P. Nigam, D. Singh, R. Marchant, Microbial decolorization of textile-dye-containing effluents: a review, Bioresour. Technol., 58 (1996) 217–227.

[24] M.N.V. Ravi Kumar, T.R. Sridhari, K.D. Bhavani, P.K. Dutta, Trends in color removal from textile mill effluents, Colorage, 40 (1998) 25–34.

[25] W.G. KUO, Decolorizing dye waste water with Fenton reagent, Water. Res., 26 (1992) 881–886.

[26] P.W. Wong, T.T. Teng, N. Abdul, R Nik, Efficiency of the coagulation-flocculation method for the treatment of dye mixtures containing disperse and reactive dye, Water Qual. Res. J., 42 (2007) 54–62.

[27] W. Zhang, C. Zhou, W. Zhou, A. Lei, Q. Zhang, Q. Wan, B. Zou, Fast and considerable adsorption of methylene blue dye onto graphene oxide, Bull. Environ. Contam. Toxicol., 87 (2011) 86–90.

[28] G. Xie, P. Xi, H. Liu, F. Chen, L. Huang, Y. Shi, J. Wang, A facile chemical method to produce superparamagnetic graphene oxide–Fe_3O_4 hybrid composite and its application in the removal of dyes from aqueous solution, J. Mater. Chem., 22 (2012) 1033–1039.

[29] G.K. Ramesha, A.V. Kumara, H.B. Muralidhara, S. Sampath, Graphene and graphene oxide as effective adsorbents toward anionic and cationic dyes, J. Colloid Interface Sci., 361 (2011) 270–277.

[30] A. Naseri, R. Barati, F. Rasoulzadeh, M. Bahram, Studies on adsorption of some organic dyes from aqueous solution onto graphene nanosheets, Iran, J. Chem. Chem. Eng., 34 (2015) 33–42.

[31] M. Iqbal, A. Abdala, Thermally reduced graphene: synthesis, characterization and dye removal applications, RSC Adv., 3 (2013) 24455.

[32] J.H. Deng, X.R. Zhang, G.M. Zeng, J.L. Gong, Q.Y. Niu, J. Liang, Simultaneous removal of Cd(II) and ionic dyes from aqueous solution using magnetic graphene oxide nanocomposite as an adsorbent, Chem. Eng. J., 226 (2013) 189–200.

[33] R. Tovar-Gómez, D.A. Rivera-Ramírez, V. Hernández-Montoya, A. Bonilla-Petriciolet, C.J. Durán-Valle, M.A. Montes-Morán, Synergic adsorption in the simultaneous removal of acid blue 25 and heavy metals from water using a $Ca(PO_3)_2$-modified carbon, J. Hazard. Mater., 199–200 (2012) 290–300.

[34] K. Atrak, A. Ramazani, S.T. Fardood, Green synthesis of $Zn_{0.5}Ni_{0.5}AlFeO_4$ magnetic nanoparticles and investigation of their photocatalytic activity for degradation of reactive blue 21 dye, Environ. Technol., (2019) DOI: 10.1080/09593330.2019.1581841.

[35] Y. Zhu, S. Murali, W. Cai, X. Li, J.W. Suk, J.R. Potts, R.S. Ruoff, Graphene and graphene oxide: synthesis, properties and applications, Adv. Mater., 22 (2010) 3906–3924.

[36] W. Chen, L. Yan, P.R. Bangal, Chemical reduction of graphene oxide to graphene by sulfur-containing compounds, J. Phys. Chem. C, 114 (2010) 19885–19890.

[37] W. Chen, L. Yan, P.R. Bangal, Preparation of graphene by the rapid and mild thermal reduction of graphene oxide induced by microwaves, Carbon, 48 (2010) 1146–1152.

[38] R. Rezaee, S. Nasseri, A.H. Mahi, R. Nabizadeh, S.A. Mousavi, A. Rashidi, A. Jafari, S. Nazmara, Fabrication and characterization of a polysulfone-graphene oxide nanocomposite membrane for arsenate rejection from water, J. Environ. Health Sci. Eng., 13 (2015) 61.

[39] J.I. Paredes, S. Villar-Rodil, P. Solis-Fernandez, A. Martinez-Alonso, J.M.D. Tascon, Atomic force and scanning tunneling microscopy imaging of graphene nanosheets derived from graphite oxide, Langmuir, 25 (2009) 5957–5968.

[40] L.G.B. Machuno, A.R. Oliveira, R.H. Furlan, A.B. Lima, L.C. Morais, R.V. Gelamo, Multilayer Graphene films obtained by dip coating technique, Mater. Res., 18 (2015) 775–780.

[41] M. Ghorbani, H. Abdizadeh, M.R. Golobostanfard, Reduction of graphene oxide via modified hydrothermal method, Procedia Mater. Sci., 11 (2015) 326–330.

[42] N.D. Luong, N. Pahimanolis, U. Hippi, J.T. Korhonen, J. Ruokolainen, L. Johansson, J. Namd, J. Seppala, Graphene/cellulose nanocomposite paper with high electrical and mechanical performances, J. Mater. Chem., 21 (2011) 13991–13998.

[43] G.G. Wallace, R.B. Kaner, M. Muller, S. Gilje, D. Li, Processable aqueous dispersions of graphene nanosheets, Nature Nanotech., 3 (2008) 101–105.

[44] P. Bartezak, M. Norman, L. Klapiszewski, N. Karwanska, M. Kawalec, M. Baczynska, M. Wysokowski, J. Zdarta, F. Ciesielczyk, T. Jesionowski, Removal of nickel(II) and lead(II) ions from aqueous solution using peat as a low-cost adsorbent: a kinetic and equilibrium study, Arab. J. Chem., 11 (2018) 1209–1222.

[45] P. Nuengmatcha, S. Chanthai, Adsorption capacity of the As-synthetic graphene oxide for the removal of alizarin red S dye from aqueous solution, Orient. J. Chem., 32 (2016) 1399–1410.

[46] A. Shukla, Y.H. Zhang, P. Dubey, J.L. Margrave, S.S. Shukla, The role of sawdust in the removal of unwanted materials from water, J. Hazard. Mater., 95 (2002) 137–152.

[47] A. Tajiki, M. Abdouss, Synthesis and characterization of graphene oxide nano-sheets for effective removal of phthalocyanine from aqueous media, Iran. J. Chem. Chem. Eng., 36 (2017) 1–9.

[48] G. Uslu, M. Tanyol, Equilibrium and thermodynamic parameters of single and binary mixture biosorption of lead (ii) and copper (ii) ions onto pseudomonas putida: effect of temperature, J. Hazard. Mater., B, 135 (2006) 87–93.

[49] H.M.F. Freundlich, Over the adsorption in solution, J. Phys. Chem., 57 (1906) 385.

[50] Y.S. Ho, G. Mckay, Pseudo-second order model for sorption processes, Process Biochem., 34 (1999) 451–465.

[51] A. Elsagh, O. Moradi, A. Fakhri, F. Najafi, R. Alizadeh, V. Haddadi, Evaluation of the potential cationic dye removal using adsorption by graphene and carbon nanotubes as adsorbents surfaces, Arab. J. Chem., 10 (2017) S2862–S2869.

[52] C.R. Minitha, M. Lalitha, Y.L. Jeyachandran, L. Senthilkumar, R.T.R. Kumar, Adsorption behaviour of reduced graphene oxide towards cationic and anionic dyes: Co-action of electrostatic and $\pi - \pi$ interactions, Mater. Chem. Phys., (2017) DOI: 10.1016/j.matchemphys.2017.03.048.